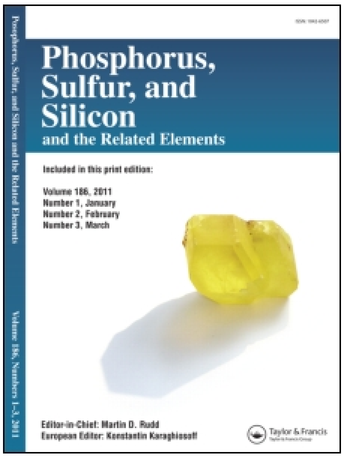

**Phosphorus, Sulfur, and Silicon and the Related Elements**
Publication details, including instructions for authors and subscription information:
http://www.informaworld.com/smpp/title~content=t713618290

# MULTINUCLEAR MAGNETIC RESONANCE STUDY OF GROUP 14-SUBSTITUTED SULFUR DIIMIDES, AND THE MOLECULAR STRUCTURES OF DI-*tert*-BUTYL-, BIS(TRIPHENYLSILYL)- AND N-TRIMETHYLSILYL-N'-TRIPHENYLSILYL SULFUR DIIMIDE

Max Herberhold[a]; Silke Gerstmann[a]; Wolfgang Milius[a]; Bernd Wrackmeyer[a]; Horst Borrmann[b]
[a] Laboratorium für Anorganische Chemie, Universität Bayreuth, Bayreuth, Germany [b] Max-Planck-Institut für Festkörperforschung, Stuttgart, Germany

**To cite this Article** Herberhold, Max , Gerstmann, Silke , Milius, Wolfgang , Wrackmeyer, Bernd and Borrmann, Horst(1996) 'MULTINUCLEAR MAGNETIC RESONANCE STUDY OF GROUP 14-SUBSTITUTED SULFUR DIIMIDES, AND THE MOLECULAR STRUCTURES OF DI-*tert*-BUTYL-, BIS(TRIPHENYLSILYL)- AND N-TRIMETHYLSILYL-N'-TRIPHENYLSILYL SULFUR DIIMIDE', Phosphorus, Sulfur, and Silicon and the Related Elements, 112: 1, 261 — 279

**To link to this Article: DOI:** 10.1080/10426509608046369

**URL:** http://dx.doi.org/10.1080/10426509608046369

*Phosphorus, Sulfur, and Silicon*, 1996, Vol. 112, pp. 261–279
Reprints available directly from the publisher
Photocopying permitted by license only

# MULTINUCLEAR MAGNETIC RESONANCE STUDY OF GROUP 14-SUBSTITUTED SULFUR DIIMIDES, AND THE MOLECULAR STRUCTURES OF DI-*tert*-BUTYL-, BIS(TRIPHENYLSILYL)- AND N-TRIMETHYLSILYL-N′-TRIPHENYLSILYL SULFUR DIIMIDE

MAX HERBERHOLD,* SILKE GERSTMANN, WOLFGANG MILIUS and BERND WRACKMEYER*

*Laboratorium für Anorganische Chemie, Universität Bayreuth, D-95440 Bayreuth, Germany*

and

HORST BORRMANN

*Max-Planck-Institut für Festkörperforschung, Heisenbergstr. 1, D-70569 Stuttgart, Germany*

*(Received November 14, 1995)*

Sulfur diimides of the type R(NSN)R′ (**1**–**19**, **2a**–**9a**, **12a**–**17a**, **20a**, **3b**–**16b**, **20b**) were investigated by $^{15}N$, $^{29}Si$ and $^{119}Sn$ NMR at variable temperature in order to determine their preferred configuration (E/Z, Z/E, E/E or Z/Z) in solution. All sulfur diimides studied are highly fluxional at room temperature. In some cases with N$^t$Bu groups, the presence of two isomers could be demonstrated. In solution, the E position is preferred for a silyl group, as shown, e.g., for N-*tert*-butyl-N′-trimethylsilyl sulfur diimide (**2a**). In the case of one germyl group, there is little preference of either E or Z position, whereas stannyl groups prefer to be in Z position. The situation in solution may differ considerably from the configurations determined in the solid state. Single crystal X-ray analyses were carried out for di-*tert*-butyl- (**1**), bis(triphenylsilyl)- (**7**) and N-trimethylsilyl-N′-triphenylsilylsulfur diimide (**7b**). All three molecules adopt the Z/E configuration in the crystal. Solid-state $^{29}Si$ CP/MAS NMR spectra indicate that in the case of **7** the bulk material consists of two isomers, one with the Z/E configuration, as found from the X-ray analysis, and a second one, most likely with E/E configuration. Solid-state $^{119}Sn$ CP/MAS NMR spectra of bis(trimethylstannyl)sulfur diimide (**4**) prove that there is only one tin site in the solid state, most likely the isomer with Z/Z configuration. In contrast, solid-state $^{119}Sn$ NMR spectra of bis(triphenylstannyl)sulfur diimide (**6**) suggest that it exists solely as isomer with Z/E configuration.

*Key words:* Sulfur diimides, silyl-, germyl- and stannyl-substituted, $^{15}N$, $^{29}Si$, $^{119}Sn$ NMR, solid-state $^{29}Si$, $^{119}Sn$ CP/MAS NMR, X-ray analyses.

## INTRODUCTION

X-ray structure analyses have shown that all four possible configurations of sulfur diimides, R(NSN)R′, can exist in the solid state,[1] whereas in solution most sulfur diimides appear to be fluxional systems and undergo fast E/Z ⇌ Z/E isomerization.[2]

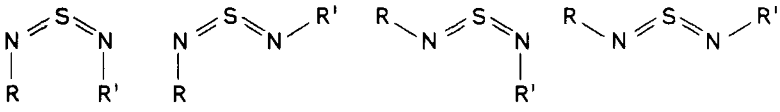

(Z/Z) (Z/E) (E/Z) (E/E)

With respect to the rich chemistry of sulfur diimides,[2] in particular of organometallic-substituted sulfur diimides,[3] it is important to determine their preferred configuration in solution and to compare this information, wherever possible, with structural data for the solid state. Clearly, NMR measurements both in solution and in the solid state, together with direct structural data from X-ray analyses, will serve this purpose. It turns out, however, that $^1$H and $^{13}$C NMR data of the substituents R and R′, with the exception of those for R or R′ = $^t$Bu,[4] are not very helpful in this respect. In previous work,[4–6] we have already applied $^{15}$N NMR with considerable success to the problem of configurational assignment in solution. We have now studied numerous symmetrically (R = R′) and unsymmetrically substituted (R ≠ R′) sulfur diimides[5a] (numbering in Scheme I), focusing on $^{15}$N, $^{29}$Si and $^{119}$Sn NMR in solution. In some cases, solid-state $^{13}$C, $^{29}$Si and $^{119}$Sn CP/MAS NMR spectra were measured. Furthermore the molecular structures of di-*tert*-butylsulfur diimide (**1**), bis(triphenylsilyl)sulfur diimide (**7**) and N-trimethylsilyl-N′-triphenylsilylsulfur diimide (**7b**) were determined by X-ray analysis. The synthesis of most compounds studied here has been described,[5] and new compounds (**15–19**, **15a–17a**, **20a**, **15b–16b**, **20b**) were prepared by following the established methods.

## RESULTS AND DISCUSSION

The Tables I, II and III list $^{15}$N, $^{29}$Si and $^{119}$Sn NMR data for the compounds $^t$Bu(NSN)ER$^1_2$R$^2$, Me$_3$Si(NSN)ER$^1_2$R$^2$ and R$^2$R$^1_2$E(NSN)ER$^1_2$R$^2$, respectively.

The $^{15}$N NMR spectra were measured by using one of the following methods: (i) $^1$H inverse-gated decoupling for suppression of the NOE; (ii) $^1$H coupled $^{15}$N; (iii) non-refocused INEPT pulse sequence; (iv) refocused INEPT pulse sequence[7] with $^1$H decoupling (polarization transfer based on $^3J(^{15}N^1H)$). The latter technique is particularly efficient if N$^t$Bu, NSiMe$_3$, NSiMe$_2$ and NGeMe$_3$ groups are present and $^3J(^{15}N^1H)$ is assumed to be 2.0–2.5 (N$^t$Bu) or 1.0–1.8 (all other groups). Selective $^1$H decoupling allows to correlate $^{15}$N and $^1$H resonances in 1D experiments. Under favorable conditions, 2D heteronuclear $^{15}$N/$^1$H shift correlations can also be carried out. These polarization transfer experiments may become much less efficient if scalar relaxation of the first kind (induced by dynamic processes such as configurational isomerization) shortens the transverse relaxation time T$_2$($^1$H) and/or T$_2$($^{15}$N). Frequently, these dynamic processes are very fast as compared to the NMR time scale (e.g., the Z/E $\rightleftharpoons$ E/Z isomerization of many silyl- or stannyl-substituted sulfur diimides) and do not hamper the application of polarization transfer.

Unfortunately most of the sulfur diimides are liquids, precluding a systematic application of solid-state NMR techniques. A further difficulty arises with natural abundance CP/MAS $^{15}$N NMR spectra of the sulfur diimides. It turns out that the $T_{1\rho}(^1H,^{15}N)$ values are extremely unfavorable[6b] for efficient cross polarization. There were no experimental problems in measuring $^{13}$C, $^{29}$Si or $^{119}$Sn NMR spectra of the

**Scheme I:**

Numbering scheme for the sulfur diimides $R^2R^1_2E(NSN)ER^1_2R^2$ and $R(NSN)ER^1_2R^2$ (R = $^t$Bu, SiMe$_3$).

| $ER^1_2R^2$ = | $R^2R^1_2E(NSN)ER^1_2R^2$ | $R(NSN)ER^1_2R^2$ | $R(NSN)ER^1_2R^2$ |
|---|---|---|---|
| | | R = $^t$Bu | R = SiMe$_3$ |
| $^t$Bu | 1 | 1 | 2a |
| SiMe$_3$ | 2 | 2a | 2 |
| GeMe$_3$ | 3 | 3a | 3b |
| SnMe$_3$ | 4 | 4a | 4b |
| SnBu$_3$ | 5 | 5a | 5b |
| SnPh$_3$ | 6 | 6a | 6b |
| SiPh$_3$ | 7 | 7a | 7b |
| SiMe$_2$H | 8 | 8a | 8b |
| Si$^t$Bu$_2$H | 9 | 9a | 9b |
| SiPh$_2$Me | 10 | - | 10b |
| SiMe$_2$Ph | 11 | - | 11b |
| SiMe$_2$$^t$Bu | 12 | 12a | 12b |
| SiPh$_2$$^t$Bu | 13 | 13a | 13b |
| SiMe$_2$SiMe$_3$ | 14 | 14a | 14b |
| SiMe$_2$C≡CPh | 15 | 15a | 15b |
| SnBz$_3$ | 16 | 16a | 16b |
| SiMe$_2$Cl | 17 | 17a | - |
| SiMe$_2$C≡CBu | 18 | - | - |
| SiMe$_2$Mes | 19 | - | - |
| SiMe$_2$SiMe$_2$(NSN)R | - | 20a | 20b |

solid sulfur diimides. Therefore, $^{13}$C, $^{29}$Si and $^{119}$Sn CP/MAS NMR spectra of the few crystalline solid compounds (**4**, **6**, **7**, **7a**, **7b**) are the major link for a comparison of the structures in the solid state and in solution.

## CHEMICAL SHIFTS $\delta^{15}$N, $\delta^{29}$Si AND $\delta^{119}$Sn

*N-tert-butyl-substituted sulfur diimides, $^t$Bu(NSN)ER$^1_2$R$^2$* (**1**, **2a**–**9a**, **12a**–**17a**, **20a**). The Z/E configuration of $^t$Bu(NSN)$^t$Bu (**1**) in solution at low temperature has been firmly established by early $^1$H NMR studies,[8a] by $^1$H and $^{13}$C NMR,[8b] and more recently by $^{15}$N NMR.[5a] This structure is now also confirmed for the solid state by X-ray analysis (*vide infra*). The set of $\delta^{15}$N data of N,N′-dialkyl sulfur diimides,[6a]

TABLE I

$^{15}$N, $^{29}$Si and $^{119}$Sn NMR data[a] of the *tert*-butyl substituted sulfur diimides, $^t$Bu(NSN)ER$^1_2$R$^2$

| Compound | I | $\delta^{15}$N | | $\delta^{29}$Si/$\delta^{119}$Sn | $^{15}$N[b] |
|---|---|---|---|---|---|
| | [%] | N$^t$Bu | NER$^1_2$R$^2$ | (ER$^1_2$R$^2$) | |
| **2a** $^t$Bu(NSN)SiMe$_3$[c] | | | | | |
| Z E | 95 | -60.5[d] | -65.9[d] | +1.7 | A |
| E Z | 5 | +34.1 | -141.5 | +2.4 | |
| **3a** $^t$Bu(NSN)GeMe$_3$[e] | | | | | |
| Z E | 70 | -68.5 | -46.0 | --- | A |
| E Z | 30 | +17.1 | -128.7 | --- | |
| **4a** $^t$Bu(NSN)SnMe$_3$[c] | | | | | |
| Z E | 25 | -65.4 | -38.9 | +53.6 | B |
| E Z | 75 | +14.1 | -121.0[f] | +41.2 | |
| **5a** $^t$Bu(NSN)SnBu$_3$[e] | | | | | |
| Z E | 20 | -61.1 | -48.0 | +36.3[g] | B |
| E Z | 80 | +12.7 | -122.4 | +33.1[h] | |
| **6a** $^t$Bu(NSN)SnPh$_3$[c] | | | | | |
| Z E | 20 | -57.0[i] | -55.4[i] | -114.6[j] | B |
| E Z | 80 | +17.3 | -136.3 | -116.2 | |
| **7a** $^t$Bu(NSN)SiPh$_3$[c] | | | | | |
| Z E | 100 | -80.7[l] | -51.1 | -21.6[m] | A,F |
| **8a** $^t$Bu(NSN)SiMe$_2$H | | | | | |
| Z E | 100 | -57.8 | -73.8[n] | -15.2 | A |
| **9a** $^t$Bu(NSN)Si$^t$Bu$_2$H | | | | | |
| Z E | 100 | -55.6 | -80.3[o] | +1.0 | A,D |
| **12a** $^t$Bu(NSN)SiMe$_2$$^t$Bu[e] | | | | | |
| Z E | 100 | -58.8 | -71.4 | +5.7 | A |
| **13a** $^t$Bu(NSN)SiPh$_2$$^t$Bu | | | | | |
| Z E | 100 | -52.6 | -80.7 | -12.7 | B |
| **14a** $^t$Bu(NSN)SiMe$_2$SiMe$_3$ | | | | | |
| Z E [c;p] | 80 | -60.3 | -66.0 | -7.2; -19.9 | A |
| E Z [q] | 20 | +31.4 | -137.8 | -6.6; -22.9 | |
| **15a** $^t$Bu(NSN)SiMe$_2$C≡CPh[e] | | | | | |
| Z E | 100 | -55.1 | -76.6 | -23.6 | A |
| **16a** $^t$Bu(NSN)SnBz$_3$[c] | | | | | |
| Z E | 15 | n.o. | n.o. | -36.2[r] | B |
| E Z | 85 | +15.5 | -124.8 | -50.3[s] | |
| **17a** $^t$Bu(NSN)SiMe$_2$Cl | | | | | |
| Z E | 100 | -52.1[t] | -81.7[t] | +4.6 | A |
| **20a** see text [c] | | | | | |
| (Z/E/E/Z) | 70 | -58.1(Z) | -69.0(E) | -10.3 | B |
| (Z/E/Z/E) | 30 | -60.8(Z) | -66.8(E) | -9.8 | |
| | | +32.6(E) | 139.7(Z) | -9.7 | |

[a] In $C_6D_6$, measured at +27°C; ; n.o. = not observed; if not mentioned otherwise the assignment of the $^{15}$N resonance of N$^t$Bu is always based upon the refocused INEPT pulse sequence with $^1$H decoupling ($^3J(^{15}N^1H)$ was assumed to be 2.0-2.5 Hz).

TABLE I (*Continued*)

[b] $^{15}$N NMR methods: **A** = refocused INEPT pulse sequence with $^{1}$H decoupling; **B** = $^{1}$H-inverse gated; **C** = $^{15}$N{$^{1}$H}; **D** = non refocused INEPT pulse sequence with $^{1}$H decoupling; **E** = refocused INEPT pulse sequence with selective $^{1}$H decoupling; **F** = $^{1}$H coupled $^{15}$N.

[c] In toluene[$d_8$], measured at -40°C.

[d] Assignment based upon heteronuclear 2D{$^{15}$N$^{1}$H} NMR experiments.

[e] In toluene[$d_8$], measured at -30°C.

[f] $^{1}J(^{119}Sn^{15}N)$ = 144.6 Hz.

[g] $h_{1/2}$ = 10 Hz; $\delta^{119}$Sn (27°C) = 31.9 ($h_{1/2}$ = 70 Hz); $\delta^{119}$Sn (-20°C) = 35.5 ($h_{1/2}$ = 25 Hz); $\delta^{119}$Sn (-65°C) = 36.1 ($h_{1/2}$ = 10 Hz).

[h] $h_{1/2}$ = 10 Hz; $\delta^{119}$Sn (-20°C) = 32.4 ($h_{1/2}$ = 25 Hz); $\delta^{119}$Sn (-65°C) = 34.0 ($h_1$ = 10 Hz).

[i] No assignment.

[j] $h_{1/2}$ = 25 Hz; $\delta^{119}$Sn (-50°C) = -113.0 ($h_{1/2}$ = 23 Hz).

[k] $h_{1/2}$ = 14 Hz; $\delta^{119}$Sn (-50°C) = -115.0 ($h_{1/2}$ = 18 Hz).

[l] $\delta^{15}$N(+27°C) = -79.3.

[m] $h_{1/2}$ = 16 Hz; $\delta^{29}$Si(-40°C) = -21.0 ($h_{1/2}$ = 2 Hz); $\delta^{29}$Si CP/MAS = -19.0 (Z), -21.8 (E).

[n] $^{2}J(^{15}N^{1}H)$ = 2.9 Hz.

[o] $\delta^{15}$N values at -10°C; $^{2}J(^{15}N^{1}H)$ = 1.8Hz; between +27°C and -5°C no $^{15}$N resonance was detected.

[p] $\delta^{29}$Si = -7.2 ($SiMe_2SiMe_3$), -19.9 ($SiMe_2SiMe_3$).

[q] $\delta^{29}$Si = -6.6 ($SiMe_2SiMe_3$), -22.9 ($SiMe_2SiMe_3$).

[r] $h_{1/2}$ = 15 Hz; $\delta^{119}$Sn (27°C) = -46.0 ($h_{1/2}$ = 140 Hz); $\delta^{119}$Sn (-20°C) = -36.8 ($h_{1/2}$ = 30 Hz); $\delta^{119}$Sn (-60°C) = -36.1 ($h_{1/2}$ = 15 Hz).

[s] $h_{1/2}$ = 15 Hz; $\delta^{119}$Sn (-20°C) = -48.6 ($h_{1/2}$ = 15 Hz); $\delta^{119}$Sn (-60°C) = -52.7 ($h_{1/2}$ = 15 Hz).

[t] In toluene[$d_8$], measured at -50°C; $\delta^{15}$N(-60°C) = -46.1 (N$^{t}$Bu), -81.7 ($NSiMe_2Cl$), at -60°C. $^{15}$N NMR method : **B**.

nitrogen nuclear shielding calculations of sulfur diimides by GIAU methods,[6c] and the comparison of nitrogen shielding in sulfur diimides and N-sulfinylamines, R(NSO),[6a,9] considering the results of CNDO/S calculations of nitrogen nuclear shielding in N-sulfinylamines,[9] allow to assign the $^{15}$N resonance signals: The signal at higher field ($\delta^{15}N = -105.9$) belongs to the N atom with a $^{t}$Bu group in Z position and the signal at lower field ($\delta^{15}N = -6.6$) to the N atom with a $^{t}$Bu group in E position.[5a]

TABLE II

$^{15}$N, $^{29}$Si and $^{119}$Sn NMR data[a] of the trimethylsilyl substituted sulfur diimides $Me_3Si(NSN)ER^1_2R^2$

| Compound | $\delta^{15}$N | | $\delta^{29}$Si/$\delta^{119}$Sn | | $^{15}$N [b] |
|---|---|---|---|---|---|
| | $NSiMe_3$ | $NER^1_2R^2$ | $SiMe_3$ | $ER^1_2R^2$ | |
| **3b** $Me_3Si(NSN)GeMe_3$<br>Z E | -66.4 [c] | -48.7 [c] | +0.1 | --- | A |
| **4b** $Me_3Si(NSN)SnMe_3$<br>E Z | -47.5 [d] | -61.4 | +0.8 [e] | +42.5 [e] | B |
| **5b** $Me_3Si(NSN)SnBu_3$<br>E Z | -45.4 [f] | -64.3 [f] | -1.3 | +32.6 | B |
| **6b** $Me_3Si(NSN)SnPh_3$<br>E Z | -39.3 [g] | -73.5 [g] | +0.5 | -122.6 | B |
| **7b** $Me_3Si(NSN)SiPh_3$ | -58.3 | n.o. | +3.1 [h] | -21.6 [h] | B,C |
| **8b** $Me_3Si(NSN)SiMe_2H$ | -55.0 [f] | -66.6 [f] | +2.1 | -16.3 | A,E |
| **9b** $Me_3Si(NSN)Si^tBu_2H$<br>Z E | -71.4 | -55.6 [i] | +1.9 | -0.7 | A |
| **10b** $Me_3Si(NSN)SiPh_2Me$ | -56.3 | -61.6 | +2.7 | -14.6 | A |
| **11b** $Me_3Si(NSN)SiMe_2Ph$ | -56.3 | -59.2 | +2.4 | -6.6 | A |
| **12b** $Me_3Si(NSN)SiMe_2{}^tBu$<br>Z E | -64.4 | -53.3 | +1.7 | +6.3 | B |
| **13b** $Me_3Si(NSN)SiPh_2{}^tBu$<br>Z E | -72.3 [j] | -63.5 [j] | +2.2 | -12.3 | B |
| **14b** $Me_3Si(NSN)SiMe_2SiMe_3$<br>E Z | -38.4 [k] | -76.2 [k] | +1.4 | -7.3 [l]<br>-19.4 | B |
| **15b** $Me_3Si(NSN)SiMe_2C{\equiv}CPh$ | -58.4 | -62.4 | +3.0 | -24.0 | A |
| **16b** $Me_3Si(NSN)SnBz_3$<br>E Z | -43.6 | -66.9 | +0.5 | -46.1 | B |
| **20b** see text<br>(E/Z/Z/E) | -33.1 [m] | -78.2 [m] | +1.9 [n] | -10.1 [n] | A |

[a] In $C_6D_6$, measured at +27°C; n.o. = not observed; if not mentioned otherwise the assignment of the $^{15}$N resonance of $NSiMe_3$ is always based upon the refocused INEPT pulse sequence with $^1$H decoupling ($^3J(^{15}N^1H)$ was assumed to be 1.8 Hz); the $\delta^{15}$N values point to the Z position of the $SiMe_3$ groups in **9b**, **12b** and **13b**, in consequence the position of the second silyl substituent is assumed to be E.

[b] See footnote [b] in Table I.

TABLE II (*Continued*)

[c] In toluene[$d_8$], measured at -20°C; $\delta^{15}$N (27°C) = -52.3 ($NGeMe_3$), -62.9 ($NSiMe_3$).

[d] $\delta^{15}$N(-10°C) = -45.4.

[e] In toluene[$d_8$], measured at -10°C.

[f] In toluene[$d_8$], measured at -40°C.

[g] $\delta^{15}$N(-40°C) = -39.3 ($NSiMe_3$), -77.7 ($NSnPh_3$).

[h] $\delta^{29}$Si CP/MAS = +5.7 ($SiMe_3$), -21.0 ($SiPh_3$); $\delta^{13}$C CP/MAS = -0.1 ($SiMe_3$), 128.9, 130.2, 134.8, 136.3 ($SiPh_3$).

[i] $^2J(^{15}N^1H)$ = 1.4 Hz.

[j] In toluene[$d_8$], measured at -30°C.

[k] In toluene[$d_8$], measured at -50°C.

[l] $\delta^{29}$Si = -7.3 ($SiMe_2SiMe_3$), -19.4 ($SiMe_2SiMe_3$).

[m] In toluene[$d_8$], measured at -50°C; $\delta$ $^{15}$N(27°C) = -45.9 ($NSiMe_3$), -69.1 ($NSiMe_2$); $\delta^{15}$N(-40°C) = -35.6 ($NSiMe_3$), -76.2 ($NSiMe_2$); assignment based upon heteronuclear 2D{$^{15}N^1H$} NMR experiments.

[n] $\delta^{29}$Si(-65°C) = 2.4 ($SiMe_3$), -9.7 ($SiMe_2$).

The sulfur diimides $^tBu(NSN)ER^1_2R^2$ (see Table 1) frequently exist as two isomers in solution. The large difference in $^{15}$N nuclear shielding between $^t$Bu substituents in Z and in E position (analogous to $^t$Bu(NSN)$^t$Bu) enables to assign the preferred configuration. Representative examples of $^{15}$N NMR spectra are shown in Figure 1. Of the numerous possible configurations for compound **20a** only two isomers are present in which the (Z/E/E/Z) configuration (Z position of the $^t$Bu group) is preferred (70%) over the (Z/E/Z/E) configuration ($^t$Bu group both in Z and in E position). So far there is no example of a sulfur diimide with both $^t$Bu group and a second substituent in Z position.

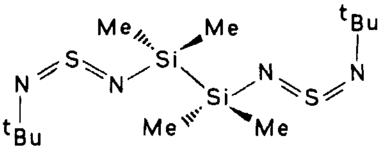

**20a**
(Z/E/E/Z)

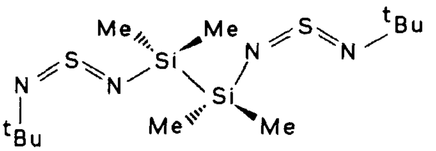

**20a**
(Z/E/Z/E)

Similarly, the $^t$Bu group in E position seems to force the second substituent into the Z position. In general, it appears that for $ER^1_2R^2$ = silyl, the (Z/E) isomer with the $^t$Bu group in Z position dominates, whereas the portion of (E/Z) isomer increases for $ER^1_2R^2$ = germyl and becomes dominant for $ER^1_2R^2$ = stannyl.

As can be seen from the $\delta^{29}$Si values of the two isomers of **2a** ($\delta^{29}$Si +1.7 and +2.4), $^{29}$Si NMR is not helpful in the configurational assignment. Somewhat larger shift differences $\Delta^{119}$Sn are found for the isomers of **4a** ($\Delta^{119}$Sn 12.4) and of **16a** ($\Delta^{119}$Sn 14.1), but the $\Delta^{119}$Sn values are again rather small in the case of the isomers

TABLE III

$^{15}$N, $^{29}$Si and $^{119}$Sn NMR data[a] of the sulfur diimides $R^2R^1_2E(NSN)ER^1_2R^2$

| Compound ($ER^1_2R^2$) | $\delta^{15}N$ $NER^1_2R^2$ | $\delta^{29}Si$ ($SiR^1_2R^2$)/ $\delta^{119}Sn$ ($SnR^1_2R^2$) | $^{15}N$ [b] |
|---|---|---|---|
| 1 ($CMe_3$) | -6.6 (E)<br>-105.9 (Z) | ---<br>--- | A,E |
| 2 ($SiMe_3$)[c] | -58.0[d] | +1.6 | A |
| 3 ($GeMe_3$) | -52.6[e] | --- | A |
| 4 ($SnMe_3$)[f] | -47.3 | +40.5 | B |
| 5 ($SnBu_3$) | -43.7 | +24.1 | A |
| 6 ($SnPh_3$) | -54.6[g] | -124.1[h] | B |
| 7 ($SiPh_3$) | --- | -21.6[i] | - |
| 8 ($SiMe_2H$) | -64.2[j] | -16.3 | A |
| 9 ($Si^tBu_2H$) | -71.9[k] | -1.1 | A |
| 10 ($SiPh_2Me$) | -61.0 | -14.1 | A |
| 11 ($SiMe_2Ph$) | -60.7[l] | -6.2 | A |
| 12 ($SiMe_2{}^tBu$) | -61.0 | +6.4 | A |
| 13 ($SiPh_2{}^tBu$) | -63.4[c] | -12.3 | B |
| 14 ($SiMe_2SiMe_3$) | -56.1[m] | -7.4; -19.5[n] | A |
| 15 ($SiMe_2C{\equiv}CPh$) | -62.4 | -23.4 | A |
| 16 ($SnBz_3$) | -50.1 | -44.1 | B |
| 17 ($SiMe_2Cl$) | -62.7 | +6.3 | F |
| 18 ($SiMe_2C{\equiv}CBu$) | -61.5 | -24.6 | A |
| 19 ($SiMe_2Mes$) | -52.4[o] | -6.9 | A |

[a] In toluene[$d_8$], measured at 27°C.

[b] See footnote [b] in Table I.

[c] In toluene[$d_8$] at -40°C.

[d] No change of the chemical shift of the $^{15}$N resonance (± 1 ppm) up to -120°C.

[e] In toluene[$d_8$], measured at 27°C; up to -55°C $\delta^{15}N$ = -52.6 (± 1 ppm); from -60°C to -110°C no $^{15}$N resonance was observed.

[f] In toluene[$d_8$], measured at -20°C; $\delta^{15}N$(-40°C) = -46.4 (broad); $\delta^{119}Sn$(CP/MAS) = 28.2.

[g] In thf-$d_8$, measured at 27°C.

[h] $h_{1/2}$ = 42 Hz; $\delta^{119}Sn$(0°C) = -122.0 ($h_{1/2}$ = 34 Hz); $\delta^{119}Sn$(-20°C) = -120.5 ($h_{1/2}$ = 32 Hz); $\delta^{119}Sn$(-40°C) = -119.5 ($h_{1/2}$ = 57 Hz); $\delta^{119}Sn$(-60°C) = -116.9 ($h_{1/2}$ = 22 Hz); $\delta^{119}Sn$(-80°C) = -115.2 ($h_{1/2}$ = 200 Hz); $\delta^{119}Sn$(CP/MAS) = -118.7 (Z), -142.0 (E).

[i] $\delta^{29}Si$ CP/MAS = -16.6 (Z), -22.8 (E).

[j] $^1J(^{29}Si^{15}N)$ = 0.4 Hz; up to -90°C $\delta^{15}N$ = -65.0 (± 1 ppm).

[k] Up to -70°C $\delta^{15}N$ = -73.0 (± 1 ppm), $^{15}$N NMR method : **B** (from -50°C to -70°C).

[l] $\delta^{15}N$(-40°C) = -60.7, $^{15}$N NMR method : **B**.

[m] Up to -50°C $\delta^{15}N$ = -56.0 (± 1 ppm).

[n] $\delta^{29}Si$ = -7.4 ($SiMe_2SiMe_3$), -19.5 ($SiMe_2SiMe_3$).

[o] $h_{1/2}$ = 1.5 Hz; $\delta^{15}N$(-50°C) = -53.1, $h_{1/2}$ = 3.0 Hz, $^{15}$N NMR method : **B**.

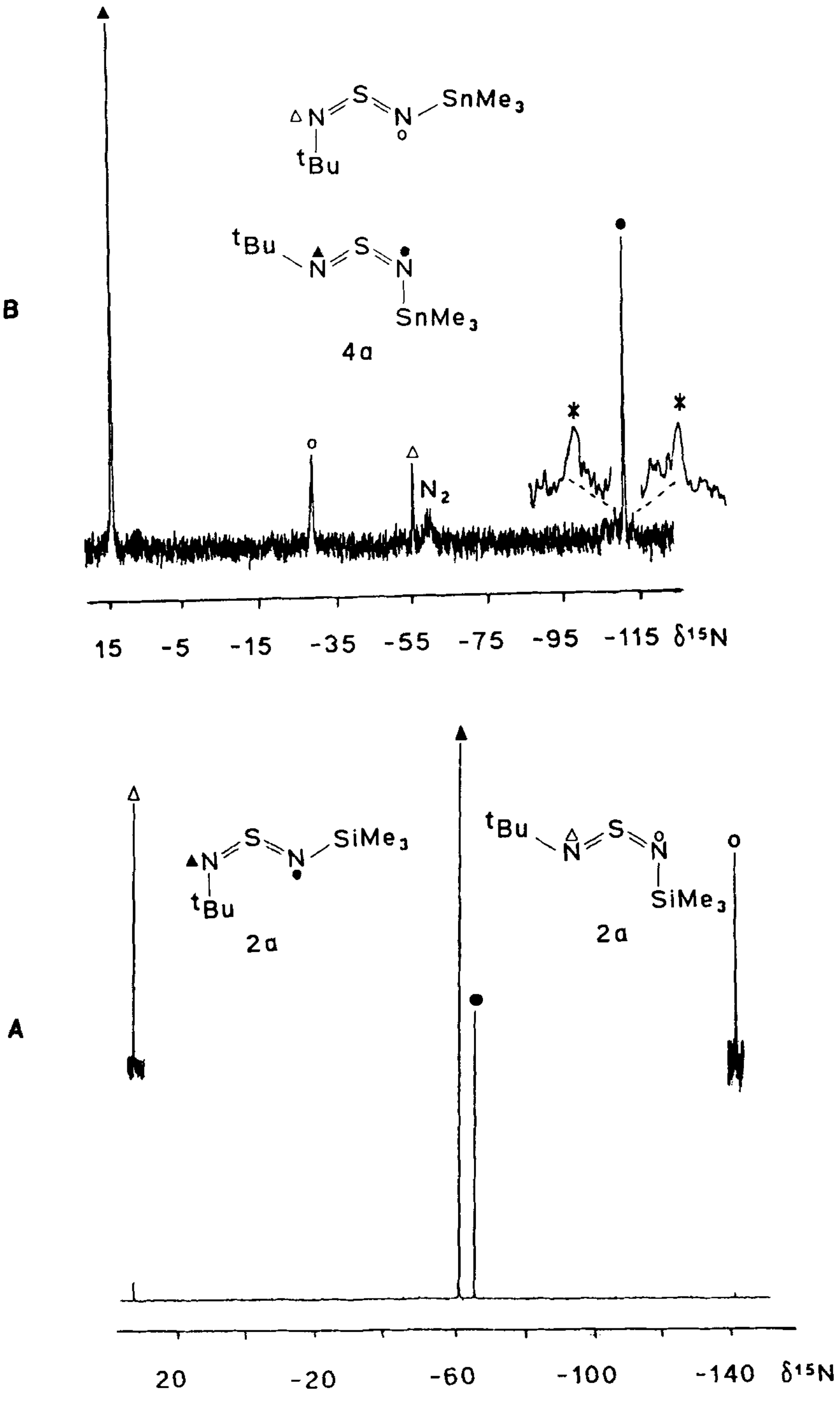

FIGURE 1 (A) 30.5 MHz $^{15}$N NMR spectrum of $^t$Bu(NSN)SiMe$_3$ (**2a**) in toluene[d$_8$], measured at −40°C, recorded using the refocused INEPT pulse sequence with $^1$H decoupling, $^3J(^{15}N^1H) = 2.5$ Hz was assumed. (B) 30.5 MHz $^{15}$N{$^1$H} NMR spectrum of $^t$Bu(NSN)SnMe$_3$ (**4a**) in toluene[d$_8$], measured at −40°C; $^{119}$Sn satellites are marked by asterisks, $^1J(^{119}Sn^{15}N) = 144.6$ Hz.

TABLE IV

Temperature dependence of $\delta^{119}$Sn values and linewidths (Hz) of the Z/E- and E/Z isomers of **4a** and **4**, and temperature dependence of $\delta^{119}$Sn values of Me$_3$Sn(NSN)SnPh$_3$

| ${}^{t}$Bu(NSN)SnMe$_3$ (**4a**) | | Me$_3$Sn(NSN)SnMe$_3$ (**4**) | Me$_3$Sn(NSN)SnPh$_3$ | | Temp. |
|---|---|---|---|---|---|
| E/Z | Z/E | [a] | Me$_3$Sn | SnPh$_3$ | [°C] |
| 56.4<br>(~1000) | 56.4<br>(~1000) | 40.5<br>(210) | 47.6 | -123.9 | +25 |
| 47.3<br>(620) | 56.7<br>(170) | 40.5<br>(83) | 49.6 | -120.7 | 0 |
| 42.8<br>(110) | 55.9<br>(50) | 40.5<br>(78) | 50.8 | -119.1 | -20 |
| 41.2<br>(290) | 53.6<br>(20) | 40.3<br>(160) | 53.0 | -116.0 | -40 |
| 37.6<br>(110) | 49.0<br>(20) | 37.4<br>(340) | 54.5 | -113.8 | -60 |
| 33.6<br>(~1100) | 48.5<br>(150) | 27.0<br>(~1000) | --- | --- | -90 |

[a] Data for a saturated solution of Me$_3$Sn(NSN)SnMe$_3$; the $\delta^{119}$Sn values of **4** and **4a** are extremly concentration and temperature dependent.

of tributyltin- **5a** ($\Delta^{119}$Sn 2.2) and triphenyltin derivatives **6a** ($\Delta^{119}$Sn 1.6). Furthermore, these $\Delta^{119}$Sn values depend markedly on concentration and temperature. Thus, it must be concluded that the $\delta^{119}$Sn data are not reliable for distinguishing configurations of stannyl sulfur diimides. However, the temperature dependence of the $\delta^{119}$Sn values and of the linewidths ($h_{1/2}$) is remarkable (Table IV). In the case of **4a** at −90°C, the $^{119}$Sn resonance of the Me$_3$Sn group in Z position is shifted by ≈23 ppm to lower frequency as compared with the broad averaged signal at 25°C. In contrast, the $^{119}$Sn NMR signal of the Me$_3$Sn group in E position remains fairly sharp and is shifted only by ≈5 ppm to lower frequency. The most likely explanation invokes weak intermolecular association as shown in **A** for the dominant isomer of **4a**. On steric grounds, the same type of interaction is expected to be weaker if the $^{t}$Bu group is in Z position (**B**).

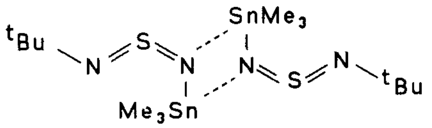

**A**

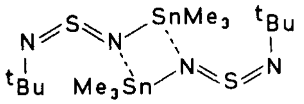

**B**

*N-Trimethylsilyl-substituted sulfur diimides, Me$_3$Si(NSN)ER$^1_2$R$^2$* (**2**, **3b–16b**, **20b**). The assignment of $^{15}$N NMR signals at high and low field to nitrogen atoms bearing the organometallic substituent in Z and E position, respectively, can also be used consistently for the N—SiMe$_3$ substituted sulfur diimides (Table II). However, the effects induced by the organometallic substituents are smaller as compared to the $^{t}$Bu group, and in many cases, the systems are more fluxional. This has already been

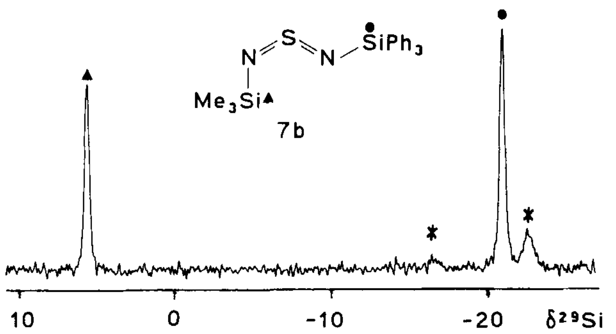

FIGURE 2 59.6 MHz $^{29}Si$ CP/MAS NMR spectrum of $Me_3Si(NSN)SiPh_3$ (**7b**); measured at 27°C, recycle delay 10 s, contact time 4.5 ms, rotation frequency 2548 Hz, 245 scans; the isotropic $\delta^{29}Si$ values are marked by $\triangle$ and $\circ$, the asterisks mark the isotropic $\delta^{29}Si$ values of $Ph_3Si(NSN)SiPh_3$ (**7**).

noted for bis(trimethylsilyl)sulfur diimide **2** and some other di(silyl)sulfur diimides such as **14b** and **20b**.[5b] For many of the examples given in Table II, $^{15}N$ NMR measurements have been carried out at various temperatures (see footnotes to Table II). The observed shifts of the $^{15}N$ NMR signals indicate that Z/E $\rightleftharpoons$ E/Z isomerization occurs still fast on the NMR time scale, although the trend of the $\delta^{15}N$ values can be used to predict the greater contribution of a particular configuration. This is indicated in Table II. The assignment given does not exclude minor contributions of opposite configurations.

*Symmetrically substituted sulfur diimides,* $R^2R^1_2E(NSN)ER^1_2R^2$ *(E = Si, Ge;* **1–3**, **7–15**, **17–19**). The $\delta^{15}N$ values of the unsymmetrically substituted sulfur diimides **14b** and **20b** clearly show that the $\delta^{15}N$ values of $Me_3Si(NSN)SiMe_3$ (**2**) and $Me_5Si_2(NSN)Si_2Me_5$ (**14**) are averaged[5b] owing to fast Z/E $\rightleftharpoons$ E/Z isomerization. This should also apply to the other di(silyl)sulfur diimides (**8–13**, **15**, **17–19**) some of which (e.g., **8**, **9**, **19**) have been studied in solution at low temperatures down to −100°C.

This situation is similar in the case of bis(trimethylgermyl)sulfur diimide **3**. The $\delta^{15}N$ value (−52.6) appears to be averaged and there is no change down to −55°C. However, we have failed to measure $^{15}N$ NMR signals of **3** between −60°C and −110°C, using INEPT or direct observation. This can be the result of severe broadening of the $^{15}N$ NMR signal owing to slower dynamic processes.

*Triphenylsilyl-substituted sulfur diimides,* $R^2R^1_2E(NSN)SiPh_3$ (**7**, **7a,b**). The results of the single crystal X-ray analyses (*vide infra*) prove that both $Ph_3Si(NSN)SiPh_3$ (**7**) and $Me_3Si(NSN)SiPh_3$ (**7b**) adopt the Z/E configuration. The solid-state $^{29}Si$ CP/MAS NMR spectrum of **7b** (Figure 2) shows two resonances (+5.7, −21.0) in a 1:1 ratio, completely in accord with the results of the X-ray analysis. In contrast, the solution-state $\delta^{15}N$ value of the $NSiMe_3$ group (−58.3) is typical of fast Z $\rightleftharpoons$ E interconversion.[5b] The fast isomerization in solution is also supported by the difference $\Delta\delta$ $^{29}Si$ 2.7 ppm between solid and liquid-state $\delta^{29}Si(SiMe_3)$ values. On the other hand, the $\delta^{29}Si(SiPh_3)$ values are nearly identical in solution (−21.6) and in the solid (−21.0), indicating the preference of the $Ph_3Si$ group for the E position also in the liquid state. Whereas **7b** exists exclusively as Z/E isomer in the solid-state, rapid isomerization between the Z/E and the E/Z isomer takes place in solution, and minor contributions to the equilibrium arising from the E/Z or even the Z/Z isomer cannot be excluded.

The solid-state $^{29}$Si CP/MAS NMR spectrum of **7** shows two resonance signals [$\delta^{29}$Si $-16.6$: $Ph_3Si$ group in Z position; $\delta^{29}$Si $-22.8$: $Ph_3Si$ group in E position as in **7b** (*vide supra*)], again in agreement with the molecular structure. However, the integral ratio is not 1:1, as expected, but rather ≈1:2, the stronger signal being at lower frequency. This ratio does not change (within the experimental error) with different contact times for cross polarization, and therefore, it suggests that the bulk of the solid material may contain another isomer in addition to the E/Z isomer of **7**. We conclude that **7** solidifies from $CH_2Cl_2$/hexane solutions as a mixture, consisting of the E/Z isomer, of which single crystals could be obtained, and the E/E isomer. This is supported by comparing the X-ray powder diagram of the bulk material of **7** (there are several additional lines which do not belong to the E/Z isomer) with that calculated from the X-ray diffraction data for the single crystal. Interestingly, a single $^{29}$Si resonance was found in solution ($\delta^{29}$Si $-21.6$). This $\delta^{29}$Si value is rather close to the solid-state $\delta^{29}$Si value assigned to the $SiPh_3$ group in E position. Thus, it appears that the E/E configuration of **7** is dominant in solution, and the Z/E configuration plays a minor role.

According to $^1$H, $^{13}$C and $^{15}$N NMR data $^t$Bu(NSN)SiPh$_3$ (**7a**) adopts the Z/E configuration in solution. The single $^{29}$Si NMR resonance ($\delta^{29}$Si $-21.6$) indicates the E position of the $Ph_3Si$ group (*vide supra*). However, the solid-state $^{29}$Si CP/MAS NMR spectrum shows two signals, one at $\delta^{29}$Si $-21.8$ ($SiPh_3$ group in E position) and another one at $\delta^{29}$Si $-19.0$ (presumably for a $SiPh_3$ group in Z position). This is another example of a sulfur diimide with a preferred Z/E configuration in solution which then crystallizes as a mixture of Z/E and E/Z isomers.

As can be seen from the NMR data, all silyl groups in the compounds **2a**, **7a–15a**, **17a**, **20a**, **3b–6b** groups seem to prefer the E position in solution. In contrast, it will be shown that the stannyl groups prefer the Z position.

*Stannyl-substituted sulfur diimides, $Me_3Sn(NSN)SnPh_3$ and $R^2R^1_2Sn(NSN)SnR^1_2R^2$* (**4–6**, **16**). In the case of $^t$Bu(NSN)SnMe$_3$ (**4a**) both the Z/E and the E/Z isomer are present in solution. From the $^{119}$Sn NMR spectra of this mixture at various temperatures (Table IV), it follows that $\delta^{119}$Sn(SnMe$_3$) ≈ +40 indicates the Z position and $\delta^{119}$Sn(SnMe$_3$) ≈ +50 the E position. The broader $^{119}$Sn NMR signals are found for the $Me_3Sn$ group in Z position, most probably as a result of weak association (A). In solution, single $^{15}$N and $^{119}$Sn resonances were found for $Me_3Sn(NSN)SnMe_3$ (**4**), pointing either to fast isomerization or to a single configuration (E/E or Z/Z). The $^{119}$Sn NMR signal of **4** at room temperature is fairly broad, depending on the concentration. It sharpens at first on cooling, then it becomes again broader, and finally it becomes extremely broad (≈1000 Hz) in concentrated toluene solutions at −90°C. The change in the $\delta^{119}$Sn values and in the linewidth (see Table IV) corresponds closely to the findings for the dominant isomer of **4a** with the $Me_3Sn$ group in Z position. The solid-state CP/MAS $^{119}$Sn NMR spectrum of **4** shows that there is only a single tin site (Figure 3) which means that we are dealing either with the E/E or the Z/Z configuration. The $\delta^{119}$Sn value of **4** in solution (of a saturated solution) at −90°C ($\delta^{119}$Sn 27.0) is very close to the isotropic solid-state $\delta^{119}$Sn value (28.2). All this leads to the conclusion that **4** exists as a Z/Z isomer in the solid state and that the Z/Z configuration is also preferred in solution, at least at low temperature.

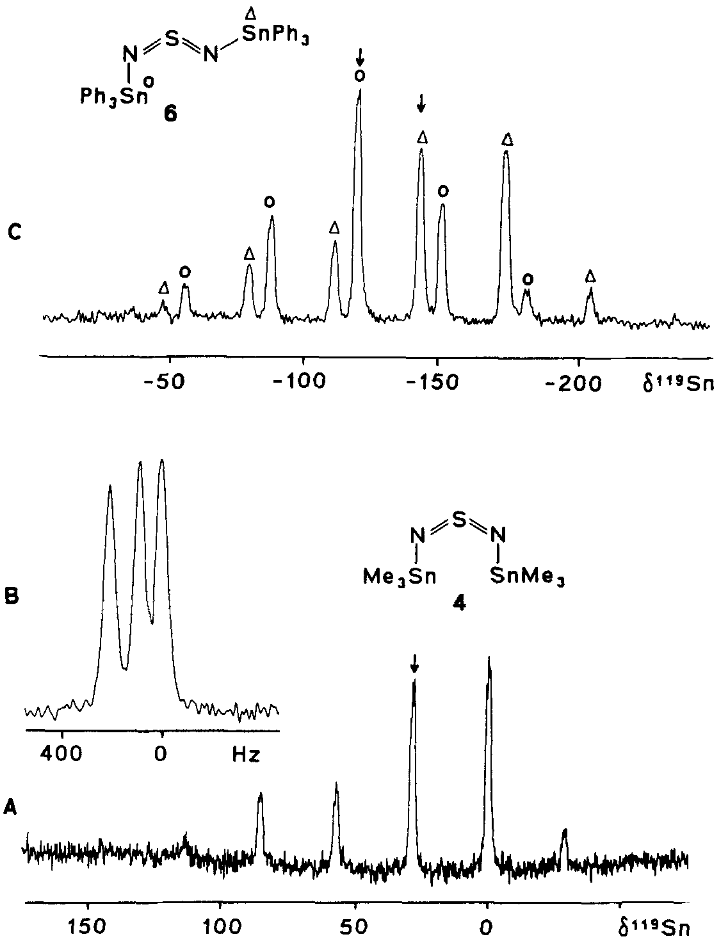

FIGURE 3 (A) 111.9 MHz $^{119}$Sn CP/MAS NMR spectrum of $Me_3Sn(NSN)SnMe_3$ (**4**); measured at 27°C, recycle delay 5 s, contact time 1 ms, rotation frequency 3192 Hz, 631 scans; the isotropic $\delta^{119}$Sn value is indicated by an arrow. (B) Enlargement of the centre band. (C) 111.9 MHz $^{119}$Sn CP/MAS NMR spectrum of $Ph_3Sn(NSN)SnPh_3$ (**6**); measured at 27°C, recycle delay 30 s, contact time 5 ms, rotation frequency 3566 Hz, 2484 scans; the isotropic $\delta^{119}$Sn values are marked by arrows.

In the case of $Me_3Sn(NSN)SnPh_3$, the $\delta^{119}Sn(SnMe_3)$ value $\approx +50$ at different temperatures (see Table IV) points to major contributions arising from isomers with the $Me_3Sn$ group in E position (see Table IV). On the other hand, the $\delta^{119}Sn(SnPh_3)$ value $\approx -118$ indicates the Z position of the $SnPh_3$ group (see the discussion of **6**). Apparently the Z/E configuration of $Me_3Sn(NSN)SnPh_3$ is preferred in solution.

In solution between +25 and −80°C, the $^{119}$Sn NMR spectrum of $Ph_3Sn(NSN)SnPh_3$ (**6**) shows only one $^{119}$Sn resonance [$\delta^{119}$Sn(25°C) −124.1]. In contrast, the solid-state $^{119}$Sn CP/MAS NMR spectrum shows two signals in a 1:1 ratio (Figure 3). Obviously **6** adopts the Z/E configuration in the solid state. The signal at lower frequency (−142.0) is assigned to the $Ph_3Sn$ group in E position, the signal at higher frequency ($\delta^{119}$Sn −118.7) to the $Ph_3Sn$ group in Z position [*in* analogy to $\delta^{29}Si(SiPh_3)$ in **7**, **7a** and **7b**]. The $\delta^{119}$Sn value of **6** in solution at −80°C

TABLE V

Experimental data related to the single crystal X-ray analyses of di-*tert*-butyl sulfur diimide (**1**), bis(triphenylsilyl) sulfur diimide (**7**) and N-trimethylsilyl-N′-triphenylsilyl sulfur diimide (**7b**)

| | **1** | **7** | **7b** |
|---|---|---|---|
| Chemical formula (mol. mass) | $C_8H_{18}N_2S$ (174.3) | $C_{36}H_{30}N_2SSi_2$ (578.9) | $C_{21}H_{24}N_2SSi_2$ (392.7) |
| Crystal | | Pale yellow; platelet | Pale yellow; platelet |
| Size | | 0.60x0.50x0.10 $mm^3$ | 0.20x0.08x0.40 $mm^3$ |
| Crystal system; space group | Triclinic; $P\bar{1}$ | Triclinic; $P\bar{1}$ | Monoclinic; $P2_1/c$ |
| Unit cell dimensions (pm) | a=597.80(14), b=929.38(18)<br>c=994.72(14)<br>$\alpha$=77.510(14)°, $\beta$=88.361(18)°<br>$\gamma$=84.662(18)° | a=987.7(2), b=1287.7(2)<br>c=1423.3(2)<br>$\alpha$=69.44(2)°, $\beta$=73.40(2)°<br>$\gamma$=88.00(2)° | a=934.3(2), b=1360.8(3)<br>c=1728.4(3)<br>$\beta$=90.99(3)° |
| V($Å^3$); Z | 524.8(2); 2 | 1620.0(5); 2 | 2197.1(8); 4 |
| Absorpt. coeff. ($mm^{-1}$) | 0.257 | 0.200 | 0.264 |
| Diffractometer | Synthex $P2_1$ | Siemens P4 | Siemens P4 |
| Radiation (pm) | Mo-$K_\alpha$, $\lambda$=71.073<br>graphite monochromator | Mo-$K_\alpha$, $\lambda$=71.073<br>graphite monochromator | Mo-$K_\alpha$, $\lambda$=71.073<br>graphite monochromator |
| Temperature (K) | 113 | 173 | 173 |
| Scan type; 2Θ range | $\omega$-2$\theta$; 2.15-35.06° | $\omega$; 3-50.0° | $\omega$; 3-50.0° |
| Measured reflections | 5594 | 6526 | 5234 |
| Indep./observed reflections | 4642/4103 | 5462/4596 [F > 3.0$\sigma$(F)] | 3843/3843 [F > 0.0$\sigma$(F)] |
| Refined parameters | 131 | 383 | 236 |
| Solution | Direct methods<br>(SHELXS-86, SHELXL-93) | Direct methods<br>(SHELXTL PLUS) | Direct methods<br>(SHELXTL PLUS) |
| Weighting scheme | $w^{-1}=s^2(F_o^2)+(0.0560P)^2+0.0021P$<br>$P=(F_o^2+2F_c^2)/3$ | $w^{-1}=\sigma^2(F)+0.0000F^2$ | $w^{-1}=\sigma^2(F)+0.0000F^2$ |
| R/$R_w$ value | 0.0806/0.0260 | 0.0560/0.0427 | 0.0560/0.0333 |
| Max./min. res. electron density ($eÅ^{-3}$) | 0.656/-0.298 | 1.15/-1.23 | 0.36/-0.35 |

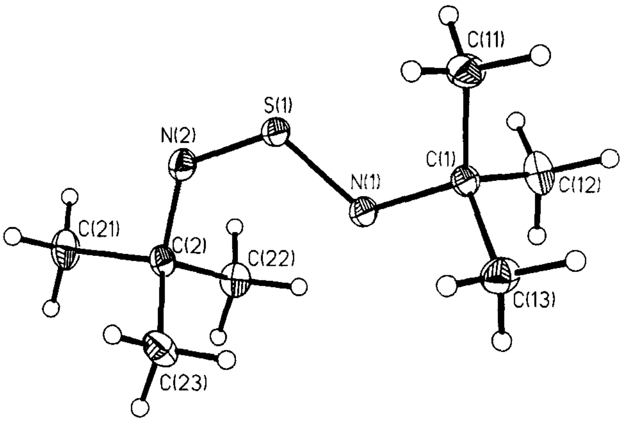

FIGURE 4 Molecular structure of $^t$Bu(NSN)$^t$Bu (1); Bond lengths [pm]: S—N(1) 154.62(6); S—N(2) 153.09(6); N(1)—C(1) 149.03(7); N(2)—C(2) 147.79(7); C(1)—C(11) 153.09(7); C(1)—C(12) 152.97(9); C(1)—C(13) 152.92(9); C(2)—C(21) 153.1(1); C(2)—C(22) 153.02(9); C(2)—C(23) 153.1(1). Bond angles [°]: N(1)—S—N(2) 117.42(3); S—N(1)—C(1) 118.18(4); S—N(2)—C(2) 127.95(4); N(1)—C(1)—C(11) 115.05(2); N(1)—C(1)—C(12) 106.45(5); N(1)—C(1)—C(13) 105.91(4); C(12)—C(1)—C(11) 109.68(5); C(13)—C(1)—C(11) 109.46(5); C(13)—C(1)—C(12) 110.19(5); N(2)—C(2)—C(21) 105.29(5); N(2)—C(2)—C(22) 110.70(5); N(2)—C(2)—C(23) 110.42(5); C(21)—C(2)—C(23) 109.90(5); C(22)—C(2)—C(21) 109.88(5); C(22)—C(2)—C(23) 110.52(5).

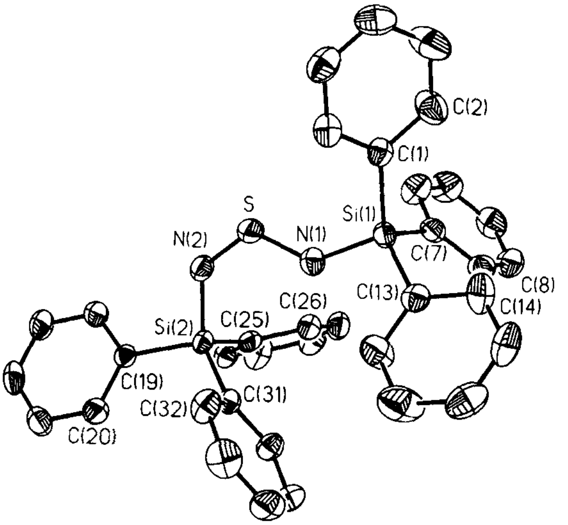

FIGURE 5 Molecular structure of $Ph_3Si(NSN)SiPh_3$ (7); Bond lengths [pm]: S—N(1) 150.6(3); S—N(2) 150.8(3); N(1)—Si(1) 173.9(3); N(2)—Si(2) 176.1(2). Bond angles [°]: N(1)—S—N(2) 117.6(1); S—N(1)—Si(1) 133.3(1); S—N(2)—Si(2) 131.5(2).

($\delta^{119}$Sn −115.2) is very close to the isotropic solid-state $\delta^{119}$Sn value of the $Ph_3Sn$ group in Z position. This suggests a strong contribution of the Z/Z configuration in solution.

Comparing the results for the $Ph_3Si$ and $Ph_3Sn$ substituted sulfur diimides, it be-

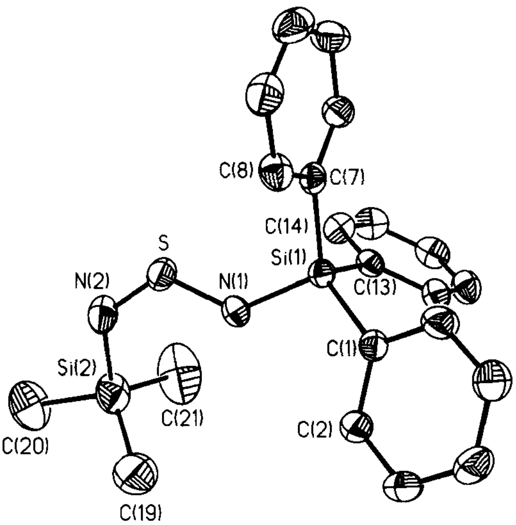

FIGURE 6 Molecular structure of $Me_3Si(NSN)SiPh_3$ (**7b**); Bond lengths [pm]: S—N(1) 151.5(2); S—N(2) 151.1(2); N(1)—Si(1) 174.2(2); N(2)—Si(2) 176.4(2). Bond angles [°]: N(1)—S—N(2) 117.4(1); S—N(1)—Si(1) 128.4(1); S—N(2)—Si(2) 127.7(1).

comes obvious that the structures of these compounds show the same trend as observed for the $Me_3Si$ and $Me_3Sn$ derivatives: The silyl group prefers the E position, whereas the stannyl group prefers the Z position. Furthermore, these examples show that the configuration of sulfur diimides in the liquid state may be quite different from that in the solid state, and that these sulfur diimides are highly fluxional in solution.

## COUPLING CONSTANTS $^1J(^{29}Si^{15}N)$, $^1J(^{119}Sn^{15}N)$

In spite of a sufficient signal-to-noise ratio, it was not possible to detect $^{29}Si$ satellites in the $^{15}N$ NMR spectra of various di(silyl) or silyl sulfur diimides.[5b] This is in agreement with extremely sharp $^{29}Si$ NMR signals which do not bear any sign of broadening owing to partially relaxed scalar $^{29}Si$—$^{14}N$ coupling. The attempt to use Hahn-echo extended (HEED)[10] pulse sequences for measuring $J(^{29}Si^{15}N)$ values in $^{29}Si$ NMR spectra also failed. Since INEPT experiments based on $^3J(^{15}NSiC^1H)$ work very well, intermolecular exchange of silyl groups can be excluded. Therefore, the values $|^1J(^{29}Si^{15}N)|$ must be very small. This is in agreement with the finding for silyl-substituted sulfinylamines, e.g. $Me_2{}^tBuSi(NSO)$, for which $^1J(^{29}Si^{15}N)$ was observed in the order of less than 1 Hz.[11] In general $^1J(^{29}Si^{15}N)$ values are positive and range from a few Hz up to 40 or 50 Hz, depending on the substituent pattern at Si.[12] The small value of $|^1J(^{29}Si^{15}N)|$ in the silyl sulfur diimides can be explained by assuming negative contributions to the Fermi contact term which arise from the presence and the nature of the lone pair of electrons at the nitrogen atom.[13]

If $^1J(^{29}Si^{15}N)$ values are close to zero, fairly large and negative values $^1J(^{119}Sn^{15}N)$ can be expected for the same type of compound.[12] Thus, $|^1J(^{119}Sn^{15}N)| = 144.6$ Hz was measured in the $^{15}N$ NMR spectrum of **4a** (see Figure 1). In other examples the signal-to-noise ratio in the $^{15}N$ NMR spectra was insufficient for reliable assignment

TABLE VI

Selected distances (pm) and bond angles (°) of the sulfur diimides $^t$Bu(NSN)$^t$Bu (**1**), $Ph_3Si(NSN)SiPh_3$ (**7**), $Me_3Si(NSN)SiPh_3$ (**7b**) and of some comparable sulfur diimides R(NSN)R′

| R/R′ configuration | d(S-N) (Z) | d(S-N) (E) | $\sphericalangle$(N-S-N) | $\sphericalangle$(S-N-R) (Z) | $\sphericalangle$(S-N-R) (E) |
|---|---|---|---|---|---|
| $^t$Bu/$^t$Bu [a]<br>Z/E | 153.09(6) | 154.62(6) | 117.42(3) | 127.95(4) | 118.18(4) |
| $SiPh_3/SiPh_3$ [a]<br>Z/E | 150.8(3) | 150.6(3) | 117.6(1) | 131.5(2) | 133.3(1) |
| $SiMe_3/SiPh_3$ [a]<br>Z/E | 151.1(2) | 151.5(2) | 117.4(1) | 127.7(1) | 128.4(1) |
| $SiMe_3/SiMe_3$[5b]<br>Z/E | 151.54(6) | 152.33(6) | 117.76(3) | 129.79(4) | 123.28(3) |
| [b]/$SiMe_3$[1c]<br>Z/E | 155.8(7) | 150.3(5) | 114.1(4) | 116.1(3) | 128.8(4) |
| $^t\mathrm{Bu_2}\overset{\overset{\mathrm{Se}}{\Vert}}{\mathrm{P}}/{}^t\mathrm{Bu_2}\overset{\overset{\mathrm{Se}}{\Vert}}{\mathrm{P}}$[16a]<br>Z/E | 150.4(4) | 152.9(4) | 116.6(2) | 137.1(2) | 118.8(2) |
| $^t\mathrm{Bu_2}\overset{\overset{\mathrm{M^{[c]}}}{\vert}}{\mathrm{P}}/{}^t\mathrm{Bu_2}\overset{\overset{\mathrm{M}}{\vert}}{\mathrm{P}}$[16b]<br>Z/E | 149.4(3) | 153.5(2) | 118.4(2) | 151.3(4) | 119.8(2) |

[a] Data from this work.

[b] R = $S\text{-}C_6H_4\text{-}4\text{-}NO_2$.

[c] M = $MnCp(CO)_2$.

of $^{117/119}$Sn satellites. The strong temperature dependence of the $^{119}$Sn NMR signals prevented the application of HEED experiments[10] to detect $^{15}$N satellites in the $^{119}$Sn NMR spectra. However, the solid-state $^{119}$Sn CP/MAS NMR spectrum of **4** (see Figure 4) shows a pattern which arises from non-averaged dipolar $^{119}$Sn—$^{14}$N interactions[14] and from scalar $^{119}$Sn—$^{14}$N coupling [$^1J(^{119}\mathrm{Sn}^{14}\mathrm{N}) \approx 85$ Hz; $^1J(^{119}\mathrm{Sn}^{15}\mathrm{N}) \approx 125$ Hz].

## X-RAY ANALYSIS.

The experimental data related to the X-ray analyses are given in Table V.[15] The molecular structures of **1**, **7** and **7b** are shown in the Figures 4–6, and the legends to the Figures 4–6 contain relevant information on bond lengths and bond angles.

A comparison of the bond angles and bond lengths of $^{t}\mathrm{Bu(NSN)}^{t}\mathrm{Bu}$ (**1**), $\mathrm{Ph_3Si(NSN)SiPh_3}$ (**7**) and $\mathrm{Me_3Si(NSN)SiPh_3}$ (**7b**), together with structural data reported for other sulfur diimides (Table VI) confirms that the structural parameters of **1**, **7** and **7b** are in the expected range. The SN bond distances (between 150 and 154 pm) are typical for S=N double bonds, and the bond angles N—S—N (117.42°; 117.6° and 117.4°) are characteristic of sulfur diimides with Z/E configuration. It is apparent from the data in Table VI that the bond angle S—N—El (element El = C, Si, P, S) of the Z-substituent is mainly determined by steric requirements since the more bulky groups cause a larger bond angle. In contrast, there are convincing examples that in the E position the bond angles S—N—El (El = C, Si, P) do not respond to the bulkiness of the substituent: (i) There is a difference of 5.5° for the E fragments $\mathrm{SNSiMe_3}$ in $\mathrm{Me_3Si(NSN)SiMe_3}$ (**2**) and $\mathrm{Me_3Si(NSN)S{-}C_6H_4{-}4{-}NO_2}$; (ii) the bond angles S—N—P in the E fragments of $^{t}\mathrm{Bu_2(Se)P(NSN)P(Se)}^{t}\mathrm{Bu_2}$ and $^{t}\mathrm{Bu_2[(CO)_2CpMn]P(NSN)P[MnCp(CO)_2]}^{t}\mathrm{Bu_2}$ are smaller by ≈5°, ≈10° and ≈15° than the respective bond angles S—N—Si in $\mathrm{Me_3Si(NSN)SiMe_3}$ (**2**), $\mathrm{Me_3Si(NSN)SiPh_3}$ (**7b**), and $\mathrm{Ph_3Si(NSN)SiPh_3}$ (**7**), although the $^{t}\mathrm{Bu_2(Se)P}$ or $^{t}\mathrm{Bu_2[Mn(CO)Cp]P}$ group must be considered to be more bulky than a $\mathrm{SiMe_3}$ or a $\mathrm{SiPh_3}$ group. The structural data indicate that for El = Si, the bond angle S—N—El in the E fragment is widened. This appears to be a prerequisite for the fluxional character which is observed for many silyl-substituted sulfur diimides in solution.

## EXPERIMENTAL

The sulfur diimides **1**,[17] **2**,[3d,18] **3**,[19] **4**,[19a,3c] **5–6**, **8–14**, **3a**, **5a–9a**, **12a–14a**, **3b**, **5b–14b**,[5a] **17**,[18b] **20b**,[5b] **2a**,[20] **4a**[21a] and **4b**[21] were prepared as described in the literature. The sulfur diimides **15**, **16**, **19**, **15a,b**, **16a,b**,[5a] **17a**[3d] and **20a**[5b] were prepared following literature procedures closely.

$\mathrm{Me_3Sn(NSN)SnPh_3}$ was prepared by a 1:1 exchange reaction between **4** and **6** in toluene-$d_8$ in an NMR tube.

NMR spectra were recorded using Bruker AC 300, Bruker AM 500 ($^{15}$N, $^{29}$Si, $^{119}$Sn) and JEOL FX 90Q instruments ($^{29}$Si, $^{119}$Sn), equipped for multinuclear NMR at variable temperature. Conditions for INEPT[7] ($^{29}$Si, $^{15}$N NMR) were optimized according to coupling constants $^{2}J(^{29}\mathrm{Si}^{1}\mathrm{H}) \sim 7$ Hz, $^{3}J(^{15}\mathrm{N}^{1}\mathrm{H}) \sim 1.0$ to 1.8 Hz for a $\mathrm{NSiMe_2R^2}$ group and $^{3}J(^{15}\mathrm{N}^{1}\mathrm{H}) \sim 2.0$ to 2.5 Hz for a $\mathrm{N}^{t}\mathrm{Bu}$ group. In some cases, it was necessary to use $^{1}$H inverse-gated decoupling for direct $^{15}$N NMR measurements.

A Bruker MSL 300 spectrometer served for measuring the solid-state $^{13}$C, $^{29}$Si and $^{119}$Sn CP/MAS NMR spectra. Air-tight inserts[22] were used, fitting into the commercial $\mathrm{ZrO_2}$ rotor of the double bearing probe head.

Chemical shifts are given with respect to $\mathrm{Me_4Si}$ ($\delta^{29}$Si, $\Xi(^{29}\mathrm{Si}) = 19.867184$ MHz), neat $\mathrm{MeNO_2}$ ($\delta^{15}$N, $\Xi(^{15}\mathrm{N}) = 10.136767$ MHz) and $\mathrm{Me_4Sn}$ ($\delta^{119}$Sn, $\Xi(^{119}\mathrm{Sn}) = 37.290665$ MHz).

For the X-ray studies $^{t}\mathrm{Bu(NSN)}^{t}\mathrm{Bu}$ (**1**) was distilled into an X-ray capillary (diameter 0.2 mm) under high vacuum. The capillary was sealed and a cylindrical crystal (0.2 × 0.7 mm) grown *in situ* on the diffractometer, maintaining a temperature slightly below its melting point (−17°C). Crystals of $\mathrm{Ph_3Si(NSN)SiPh_3} \times 0.5\ \mathrm{CH_2Cl_2}$ (**7**) precipitated from a solution of **7** in dichloromethane/hexane at −20°C, and crystals of $\mathrm{Me_2Si(NSN)SiPh_3}$ (**7b**) were obtained from a mixture of **7b**, $\mathrm{Me_3Si(NSN)SiMe_3}$ (**2**) and **7** in hexane/ether at −20°C.

## ACKNOWLEDGEMENT

We gratefully acknowledge support of this work by the Deutsche Forschungsgemeinschaft and the Fonds der Chemischen Industrie. We thank Dr. A. Sebald for measuring numerous solid state CP/MAS NMR spectra.

## REFERENCES

1. (a) V. Busetti, *Acta Crystallogr. Sect B*, **38**, 665 (1982); (b) G. Leandri, V. Busetti, G. Valle and M. Mammi, *J. Chem. Soc. Commun.*, 413 (1970); (c) R. Jones, D. J. Williams, P. T. Wood and J. D. Woollins, *Polyhedron*, **8**, 91 (1989); (d) H. Münsterer, G. Kresze, V. Lamm and A. Gieren, *J. Org. Chem.*, **48**, 2833 (1983); (e) A. Gieren, H. Betz, T. Hübner, V. Lamm, M. Herberhold and K. Guldner, *Z. Anorg. Allg. Chem.*, **513**, 513 (1984); (f) F. P. Olsen and J. C. Barrick, *Inorg. Chem.*, **12**, 1353 (1973); (g) A. Gieren, M. Herberhold, K. Guldner and G. Süss-Fink, *Z. Anorg. Allg. Chem.*, **538**, 21 (1986).
2. (a) G. Kresze and W. Wucherpfennig, *Angew. Chem.*, **79**, 109 (1967); *Angew. Chem., Int. Ed. Engl.*, **6**, 149 (1967); (b) R. Bussas, G. Kresze, H. Münsterer and A. Schwöbel, *Sulfur Rep.*, **2**, 215 (1983).
3. (a) J. D. Woollins, "Non-Metal Rings, Cages and Clusters," p. 73 ff., Wiley, New York (1988); (b) H. W. Roesky and H. Wiezer, *Angew. Chem.*, **86**, 130 (1974); *Angew. Chem., Int. Ed. Engl.*, **13**, 146 (1974); (c) D. Hänssgen and W. Roelle, *J. Organomet. Chem.*, **56**, C14 (1973); (d) O. J. Scherer and R. Wies, *Z. Naturforsch. B*, **25**, 1486 (1970).
4. M. Herberhold, S. M. Frank and B. Wrackmeyer, *Z. Naturforsch. B*, **43**, 985 (1988).
5. (a) M. Herberhold, S. Gerstmann and B. Wrackmeyer, *Phosphorus, Sulfur and Silicon*, **66**, 273 (1992); (b) M. Herberhold, S. Gerstmann, B. Wrackmeyer and H. Borrmann, *J. Chem. Soc., Dalton Trans.*, 633 (1994); (c) M. Herberhold, C. Köhler and B. Wrackmeyer, *Phosphorus, Sulfur and Silicon*, **71**, 75 (1992).
6. (a) B. Wrackmeyer, C. Köhler and M. Herberhold, *Magn. Reson. Chem.*, **31**, 987 (1993); (b) B. Wrackmeyer, S. Gerstmann and M. Herberhold, *Magn. Reson. Chem.*, **31**, 499 (1993); (c) B. Wrackmeyer, S. Gerstmann, M. Herberhold, G. A. Webb and H. Kurosu, *Magn. Reson. Chem.*, **32**, 492 (1994).
7. (a) G. A. Morris, *J. Am. Chem. Soc.*, **102**, 428 (1980); (b) G. A. Morris and R. Freeman, *J. Am. Chem. Soc.*, **101**, 760 (1979); (c) D. P. Burum and R. R. Ernst, *J. Magn. Reson.*, **39**, 163 (1980); (d) G. A. Morris, *J. Magn. Reson.*, **41**, 185 (1980).
8. (a) J. R. Grunwell, C. F. Hoyng and J. A. Rieck, *Tetrahedron Lett.*, 2421 (1973); (b) J. Kuyper and K. Vrieze, *J. Organomet. Chem.*, **74**, 289 (1974).
9. W. Sicinska, L. Stefaniak, M. Witanowski and G. A. Webb, *Org. Magn. Reson.*, **15**, 241 (1981).
10. E. Kupce and B. Wrackmeyer, *J. Magn. Reson.*, **97**, 568 (1992).
11. B. Wrackmeyer and M. Herberhold, unpublished results.
12. B. Wrackmeyer and E. Kupce, in "Topics of Physical Organometallic Chemistry," M. Gielen, ed., Vol. 4, pp. 289–352, Freund Publishing House, Tel Aviv, 1992.
13. V. M. S. Gil and W. von Philipsborn, *Magn. Reson. Chem.*, **27**, 409 (1989).
14. R. Gobetto, R. K. Harris and D. C. Apperley, *J. Magn. Reson.*, **96**, 119 (1992), and references cited.
15. Further details of the crystal structure analyses are available on request from the Fachinformationszentrum Karlsruhe, Gesellschaft für wissenschaftlich-technische Information mbH, D-76344 Eggenstein-Leopoldshafen (Germany) on quoting the depository numbers CSD 404651 (**1**), CSD 404652 (**7**) and CSD 404653 (**7b**), the names of the authors and the journal citation.
16. (a) M. Herberhold, W. Ehrenreich, A. Gieren, H. Betz and T. Hübner, *Chem. Ber.*, **118**, 1476 (1985); (b) M. Herberhold, W. Bühlmeyer, A. Gieren and T. Hübner, *J. Organomet. Chem.*, **321**, 37 (1987).
17. D. H. Clemens, A. J. Bell and L. O'Brien, *Tetrahedron Lett.*, 1487 (1965).
18. (a) U. Wannagat and H. Kuckertz, *Angew. Chem.*, **74**, 117 (1962); (b) C. P. Warrens and J. D. Woollins, *Inorg. Synth.*, **25**, 43 (1989).
19. (a) G. Brands and A. Golloch, *Z. Naturforsch. B*, **37**, 568 (1982); (b) W. Ehrenreich, Dissertation, Universität Bayreuth, 1983.
20. I. Ruppert, V. Bastian and R. Appel, *Chem. Ber.*, **108**, 2329 (1975).
21. (a) D. Hänssgen and B. Ross, *Z. Anorg. Allg. Chem.*, **473**, 80 (1981); (b) H. W. Roesky and H. Wiezer, *Chem. Ber.*, **107**, 3186 (1974).
22. L. H. Merwin, A. Sebald, J. E. Espidel and R. K. Harris, *J. Magn. Reson.*, **84**, 367 (1989).